Nonlinear Waves.
Solitons. Autowaves. Self-Organization

Izvestiya Vysshikh Uchebnykh Zavedeniy. Applied Nonlinear Dynamics. 2024;32(1)

Article DOI: 10.18500/0869-6632-003083

Influence of additive noise on chimera and solitary states in neural networks

A. D. Ryabchenko, E. V. Rybalova✉, *G. I. Strelkova*

Saratov State University, Russia
E-mail: andreyryabchenko.2003@gmail.com, ✉rybalovaev@gmail.com, strelkovagi@sgu.ru
Received 15.08.2023, accepted 3.10.2023, available online 21.12.2023, published 31.01.2024

Abstract. The *purpose* of this work is to study numerically the influence of additive white Gaussian noise on the dynamics of a network of nonlocally coupled neuron models which are represented by FitzHugh–Nagumo oscillators. Depending on coupling parameters between the individual elements this network can demonstrate various spatio-temporal structures, such as chimera states, solitary states and regimes of their coexistence (combined structures). These patterns exhibit different responses against additive noise influences. *Methods.* The network dynamics is explored by calculating and plotting snapshots (instantaneous spatial distributions of the coordinate values at a fixed time), space-time diagrams, projections of multidimensional attractors, mean phase velocity profiles, and spatial distributions (profiles) of cross-correlation coefficient values. We also evaluate the cross-correlation coefficient averaged over the network, the mean number of solitary nodes and the probability of settling spatio-temporal structures in the neuronal network in the presence of additive noise. *Results.* It has been shown that additive noise can decrease the probability of settling regimes of solitary states and combined structures, while the probability of observing chimera states arises up to 100%. In the noisy network of FitzHugh–Nagumo oscillators exhibiting the regime of solitary states, increasing the noise intensity leads, in general case, to a decrease of the mean number of solitary nodes and the interval of coupling parameter values within which the solitary states are observed. However, there is a finite region in the coupling parameter plane, inside which the number of solitary nodes can grow in the presence of additive noise. *Conclusion.* We have studied the impact of additive noise on the probability of observing chimera states, solitary states and combined structures, which coexist in the multistability region, in the network of nonlocally coupled FitzHugh–Nagumo neuron models. It has been established that chimera states represent more stable and dominating structures among the other patterns coexisting in the studied network. At the same time, the probability of settling regimes of solitary states only, the region of their existence in the coupling parameter plane and the number of solitary nodes generally decrease when the noise intensity increases.

Keywords: nonlocal coupling, additive noise, chimera state, solitary state, FitzHugh–Nagumo model.

Acknowledgements. The research was supported by the Russian Science Foundation (project No. 20-12-00119, https://www.rscf.ru/project/20-12-00119/).

For citation: Ryabchenko AD, Rybalova EV, Strelkova GI. Influence of additive noise on chimera and solitary states in neural networks. Izvestiya VUZ. Applied Nonlinear Dynamics. 2024;32(1):121–140. DOI: 10.18500/0869-6632-003083

Introduction

Real systems inevitably contain various inhomogeneities and noises, which can have both constructive and destructive effects on the spatiotemporal dynamics of complex systems [1–8]. Noise sources can be used to stabilize and/or effectively control the operating modes of systems [2–4, 9–13], as well as to improve a number of characteristics of their functioning. Such effects include, for example, stochastic resonance [1, 6, 14] and coherent resonance [5, 15]. Recently, special attention has been paid to the influence of noise and inhomogeneities on the dynamics of networks in coupling with the discovery of new modes of partial synchronization in networks of coupled systems, namely chimera states [16–20] and solitary states [21, 22].

Chimera states were first discovered in ensembles of nonlocally coupled identical phase oscillators [16, 17]. This special spatiotemporal regime of dynamics represents an intermediate stage in the transition from the regime of coherent dynamics (synchronization) to incoherent (spatiotemporal chaos) and corresponds to the coexistence of clusters localized in the space of the ensemble with coherent (synchronized) and incoherent (desynchronized) dynamics of the ensemble oscillators. Theoretical and numerical studies have shown that chimeras can arise in networks with partial elements of different natures and with different topologies of couplings between them [16–20, 23–31]. This regime of cluster synchronization is observed not only in computer experiments, but also in real systems, for example, in power grids [32–34], in social systems [35, 36], as well as in neurobiology [37–39]. It has been shown that states similar to chimeras occur in the brain during Parkinson's disease [40], during sleep with one hemisphere in birds and mammals [41], during eye movements [42, 43], during epileptic seizures [44]. The stability of chimera states to noise disturbances was studied in networks of nonlocally coupled of oscillators with discrete [45–51] and continuous time [52–55].

Solitary states represent another important regime of spatiotemporal dynamics, which is observed in ensembles of coupled oscillators [21, 22]. This regime is characterized by the fact that most of the elements of the system are in some typical state, and the rest belong to other states (solitary), of which in the general case there may be several. In this case, elements belonging to solitary states (solitary nodes) are distributed throughout the entire ensemble randomly, but in a fairly uniform manner, that is, they do not cluster (unless special initial conditions are used), as happens in the chimera regime. Note that the number of solitary nodes increases as the coupling strength between network elements decreases. Research has shown that the emergence of solitary states is associated with the appearance of bistability in the system due to the nonlocal interaction of partial elements [21, 22]. Solitary states were discovered in networks of Kuramoto-Sakaguchi models and Kuramoto oscillators with inertia [21, 22, 56–58], systems with discrete time [28, 59, 60], FitzHugh–Nagumo oscillator systems [61–64], electrical network models [65–67] and even in experimental setups of coupled pendulums [68]. Regimes similar to solitary states also occur in neural ensembles in the brain. An example is the reaction of only individual neurons to certain stimuli [69, 70], including the so-called grandmother neurons [71, 72], the dynamics of an ensemble of neurons in the categorization task [73]. In contrast to chimera states, the robustness of solitary states to noise has been studied very little. For example, in the work [74] it was shown that the presence of noise in a ring of nonlocally coupled FitzHugh–Nagumo models leads to a transition from solitary states to "patched synchrony". The authors of the work [48] found that in the ring of nonlocally coupled Losi maps, the introduction of additive noise leads to a decrease in the interval in the parameters of the ensemble in which solitary states are observed, and to a decrease in the number of solitary nodes, but mainly at the boundaries of the region of existence of these modes. Noise modulation of control parameters leads to a qualitatively similar effect, as shown in the work [75].

This work is aimed at expanding knowledge about the effects that arise when additive noise acts on chimera and solitary states realized in ensembles of coupled nonlinear oscillators. This paper examines the dynamics of a ring of nonlocally coupled FitzHugh–Nagumo oscillators, which are classical models of neural activity. In the works [63, 76] it was shown that in such a system it is possible to establish many spatio-temporal regimes when varying the coupling parameters between partial elements. In particular, chimera and solitary states can be observed, as well as the regime of their coexistence — a combined structure — in the ensemble space. An analysis is made of the influence of additive noise on the regime of only solitary states, as well as on the regimes observed in the multistability region: chimera states, solitary states and combined structures.

1. Model studied and methods used

In this work, we study the dynamics of a ring of nonlocally coupled FitzHugh–Nagumo oscillators [77, 78] in an oscillatory mode with additive white Gaussian noise added to the slow variable (inhibitor). The network under study is described by the following system of stochastic differential equations:

$$\begin{aligned} \varepsilon\frac{du_i}{dt} &= u_i - \frac{u_i^3}{3} - v_i + \frac{\sigma}{2R}\sum_{j=i-R}^{i+R}[b_{uu}(u_j-u_i)+b_{uv}(v_j-v_i)], \\ \frac{dv_i}{dt} &= u_i + a + \frac{\sigma}{2R}\sum_{j=i-R}^{i+R}[b_{vu}(u_j-u_i)+b_{vv}(v_j-v_i)] + \sqrt{2A}\xi_i(t), \end{aligned} \tag{1}$$

where u_i and v_i are variables describing the time dynamics of the activator (fast variable) and inhibitor (slow variable), respectively, $i = 1, 2, \ldots, N = 300$ is element number in the ring. The small parameter $\varepsilon > 0$ is responsible for separating the time scales of the fast activator from the slow inhibitor (in this work the value is fixed at $\varepsilon = 0.05$), and the parameter a determines the excitability threshold. In this work, the value of this parameter is assumed to be equal to $a = 0.5$ for all elements, which corresponds to the oscillatory mode of dynamics in a single element. The R parameter specifies the number of right and left nearest neighbors that each i element is coupled with. This parameter is the radius of nonlocal coupling and is fixed at $R = 105$ in the studies. A type of a nonlocal coupling between oscillators in an ensemble (1) was proposed in the work [76] and is characterized by a coupling strength of σ. The last term in the second equation corresponds to the introduction into the system of additive noise with intensity A, ξ_i are independent sources of white Gaussian noise. The initial conditions of all elements are randomly and uniformly chosen inside the circle $u^2 + v^2 \leqslant 2^2$.

The system (1) contains not only direct couplings between elements, but also cross couplings between the activator (u) and the inhibitor (v), which are established in accordance with the rotational coupling matrix [76]:

$$B = \begin{pmatrix} b_{uu} & b_{uv} \\ b_{vu} & b_{vv} \end{pmatrix} = \begin{pmatrix} \cos\phi & \sin\phi \\ -\sin\phi & \cos\phi \end{pmatrix}, \tag{2}$$

where $\phi \in [-\pi, \pi)$. In the work [76] it was shown that in a ring of nonlocally coupled FitzHugh–Nagumo oscillators in the oscillatory mode, chimera states can be observed at $\phi = \pi/2 - 0.1$. In the work [53] this result was extended to partial elements in the excitable mode in the presence of additive noise in the system.

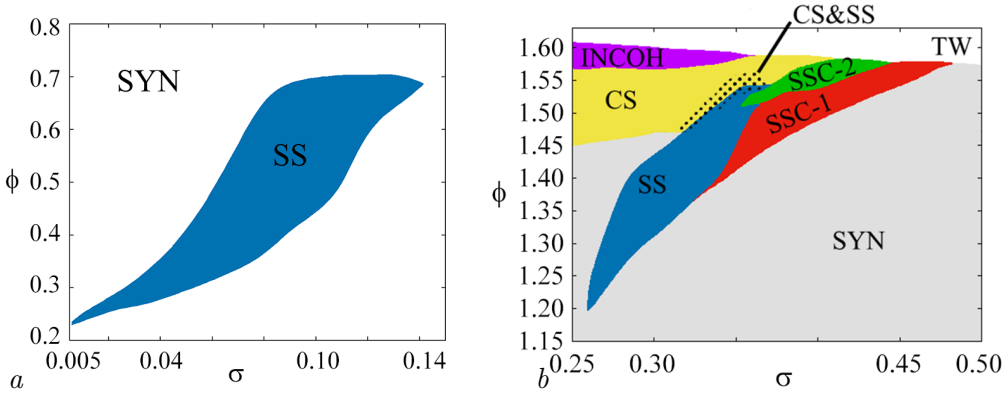

Fig 1. Diagrams of dynamical regimes in the network (1) without additive noise for weak (a) and strong (b) coupling. SYN — synchronization regime, SS — solitary state, CS — chimera state, INCOH — incoherence regime, TW — traveling wave regime, SSC-1 and SSC-2 — two different types of a solitary state chimera, CS&SS — coexistence of chimera and solitary states (combined structure). Other parameters: $\varepsilon = 0.05$, $a = 0.5$, $R = 105$, $N = 300$, $A = 0$ (color online)

In the work [63] the influence of coupling parameters σ and ϕ on the dynamics of the ring (1) in the absence of additive noise ($A = 0$) was studied. and a map of dynamic regimes was constructed (Fig. 1). Abbreviations on the map indicate all regimes observed in different regions of the parameter space. The first diagram (Fig. 1, a) is constructed for the case of weak coupling, in which two regimes are observed in the system in the region of small values of ϕ: the regime of synchronization of all elements in the ring (SYN) and solitary states (SS). The second fragment of the regime map corresponds to the case of strong coupling (Fig. 1, b). In this region, in addition to the already mentioned regimes of complete synchronization (SYN) and solitary states (SS), regimes of classical chimera states (CS) and solitary state chimeras of two types (SSC-1, SSC-2) are also observed. SSC-1 has a noncoherent cluster consisting of evenly distributed solitary nodes. Solitary state chimera type 2 (SSC-2) is also characterized by an incoherence cluster consisting of uniformly distributed solitary nodes. However, at its boundaries "steps" are formed, which are groups of solitary nodes. In addition to regions in which only chimera states and only solitary states are observed, there is a region with combined dynamics corresponding to the coexistence of chimera and solitary states (CS&SS). In what follows we will call this regime a combined structure. In the INCOH region, the dynamics of the ring are characterized by an incoherent instantaneous spatial profile and correspond to the desynchronization regime of all elements of the ensemble. The TW region corresponds to the traveling wave regime. A more detailed analysis of the dynamics of a ring of nonlocally coupled FitzHugh–Nagumo oscillators for parameters from all of the above regions is presented in the work [63].

To analyze the spatiotemporal dynamics of an ensemble of nonlocally coupled elements, snapshots (spatial distribution of the values of all dynamic variables at a fixed point in time), space-time diagrams (on the parameter plane "element number (i) - time (t))" amplitudes of partial elements) and projections of multidimensional attractors of the system onto the plane of dynamic variables are displayed in color. However, to obtain a complete picture of the evolution of various spatiotemporal regimes of the ensemble in the presence of noise impacts, it seems appropriate to calculate the cross-correlation coefficient between the ensemble elements and construct the spatial distribution of its values. The cross-correlation coefficient between the first element of the ensemble and all others is calculated using the following formula:

$$C_{1i} = \frac{\langle \tilde{u}_1 \tilde{u}_i \rangle}{\sqrt{\langle (\tilde{u}_1)^2 \rangle \langle (\tilde{u}_i)^2 \rangle}}, \quad i = 2, 3, \ldots, N, \tag{3}$$

where $\tilde{u}_i = u_i - \langle u_i \rangle$, $\langle u_i \rangle$ — averaging of u_i values over a set of realizations, which in numerical experiments was replaced by time averaging. The value (3) shows the degree of correlation or synchronization between the first element of the ensemble and all the others and varies from -1 to 1, where "1" corresponds to complete in-phase synchronization, "-1" — antiphase synchronization. In the absence of correlation between elements, this coefficient is equal to 0. Due to the fact that the correlation coefficient of solitary nodes is less than that of oscillators belonging to the coherent part of the profile, this coefficient helps to automatically detect solitary states and count the number of solitary nodes.

In addition to calculating the cross-correlation coefficient for each element (3), the cross-correlation coefficient averaged over all elements of the ensemble is also used

$$C = \frac{1}{N} \sum_{i=1}^{N} \frac{\langle \tilde{u}_1 \tilde{u}_i \rangle}{\sqrt{\langle (\tilde{u}_1)^2 \rangle \langle (\tilde{u}_i)^2 \rangle}}, \tag{4}$$

where the expression under the sum sign corresponds to the cross-correlation coefficient between the 1-th and i-th elements of (3). As was shown in the work [75], the averaged cross-correlation coefficient can be used as an additional value to estimate the number of solitary nodes in the system. In the case of coherent dynamics we have $C \to 1$; for the regime of solitary states, the value of the averaged cross-correlation coefficient decreases.

To illustrate the differences between the observed spatiotemporal structures in the ensemble of nonlocally coupled FitzHugh–Nagumo oscillators, the average phase velocity of each element in the ensemble is also calculated using the formula

$$w_i = 2\pi M_i / \Delta T, \tag{5}$$

where M_i is the number of complete rotations around the origin of coordinates performed by the i-th FitzHugh–Nagumo oscillator during the time interval ΔT [76]. In these calculations, the transition time was taken equal to $T_0 = 1000$ units of dimensionless time, and the time at which the cross-correlation coefficients and average phase velocity values were calculated was $T = 2000$.

In some cases, along with the average cross-correlation coefficient, the number of solitary nodes is directly calculated and a characteristic such as "average normalized number of solitary nodes" is used, which is defined as follows:

$$N_{\mathrm{S}} = \frac{1}{M} \sum_{M} S/N, \tag{6}$$

where S is the number of solitary nodes observed for each the initial conditions of the dynamic variables and the realization of the noise generator, N is the total number of elements in the ensemble, M is the total number of realizations used.

2. Impact of noise on modes in the multistability region

In this case, when studying the dynamics of a ring of nonlocally coupled FitzHugh–Nagumo models, the system parameters were chosen such that in the absence of noise a combined structure could be observed in the system (see Fig. 1, *b*, region "CS&SS", highlighted with dots). In addition to the combined structure, in this parameter range, depending on the initial conditions, only chimera states or regimes of only solitary states can also be realized. Moreover, the probability of establishing regimes of combined structure and purely chimera states is higher than the regime of solitary states. Fig. 2 illustrates all these three regimes in the absence of additive noise in the ensemble(1).

If only chimera states are established in the system, clusters with coherent and incoherent oscillator dynamics coexist in the ensemble space (Fig. 2, *a*), projection of a multidimensional attractor onto the (u, v) plane qualitatively coincides with the attractor typical of the FitzHugh–Nagumo oscillator, but there are small fluctuations in amplitude (Fig. 2, *a*, III). On the profile of average phase velocities, two dome-shaped dependences are observed in the region of incoherent clusters (Fig. 2, *a*, IV), and the cross-correlation coefficient in the region of incoherent clusters takes values less than one (Fig. 2, *a*, V). When a regime of only solitary states is established in the system (Fig. 2, *b*, I, II), two attractors can be distinguished in the phase portrait of all elements, where the smaller one corresponds to solitary nodes (Fig. 2, *b*, III). In this case, the values of the average phase velocities for all elements are almost equal (Fig. 2, *b*, IV), and the values of the cross-correlation coefficient of elements corresponding to solitary nodes are significantly less than those of other elements (Fig. 2, *b*, V). In the case of a combined structure (coexistence of chimeras and solitary states), all the above-described features take place (Fig. 2, *c*).

When additive noise is added to the ensemble (1), the probability of establishing (from random initial conditions) the regime of solitary states and the regime of a combined structure tends to zero, and all considered initial conditions lead to the implementation of chimera states (Fig. 3). Thus, in the presence of noise of even sufficiently low intensity $A < 2 \cdot 10^{-7}$, solitary states cease to be established in the system, and at $A > 7 \cdot 10^{-6}$ regimes of combined structures are no longer observed . Note that there is a noise intensity value, $A = 5 \cdot 10^{-6}$, at which the establishment of only chimera states and the combined structure regime is equally probable.

Fig. 4 shows the results of calculations of characteristics illustrating the dynamics of a ring of nonlocally coupled FitzHugh–Nagumo models with the addition of additive noise of different intensity. At low noise intensity, combined structures may still occur in the system, but in this case only a few solitary nodes (about 1...3) are observed in the ensemble, which is reflected in Fig. 4, *a*. A further increase in noise intensity leads to the establishment of only chimera states

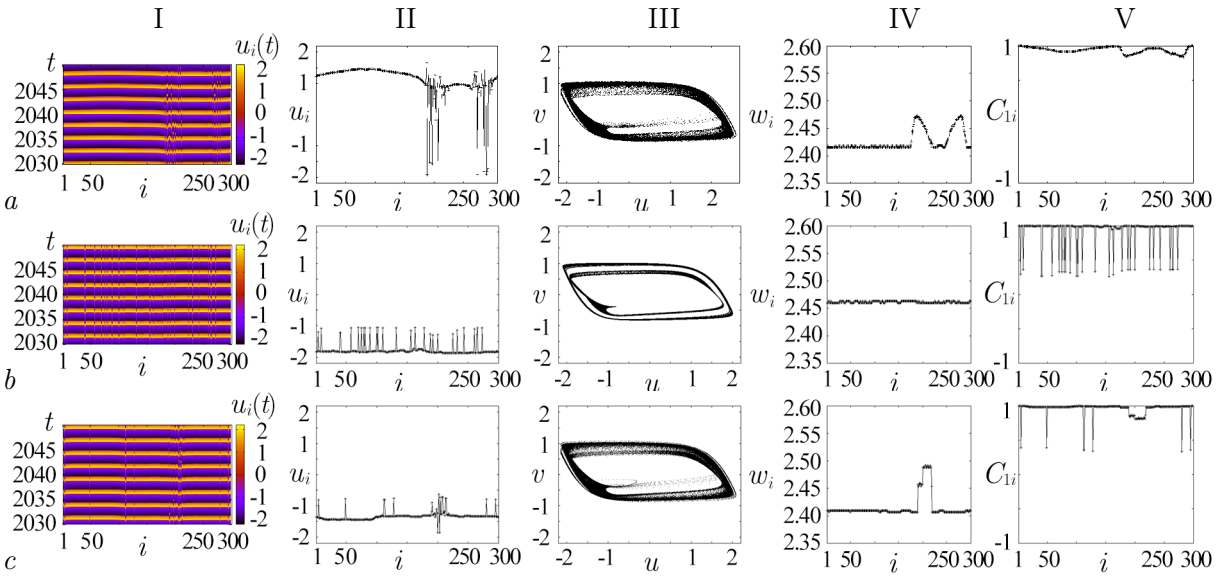

Fig 2. Dynamics of the noise-free ring network of nonlocally coupled FitzHugh–Nagumo oscillators (1) for the coupling parameters $\sigma = 0.325$, $\phi = 1.48$ and different initial distributions of dynamical variables: chimera state (*a*), solitary state (*b*), and combined structure (*c*). Space-time diagrams (column I), snapshots (column II), projections of a multidimensional attractor on the (u, v) plane (column III), mean phase velocity profiles (column IV), cross-correlation coefficient profiles (column V). Other parameters: $\varepsilon = 0.05$, $a = 0.5$, $R = 105$, $N = 300$, $A = 0$ (color online)

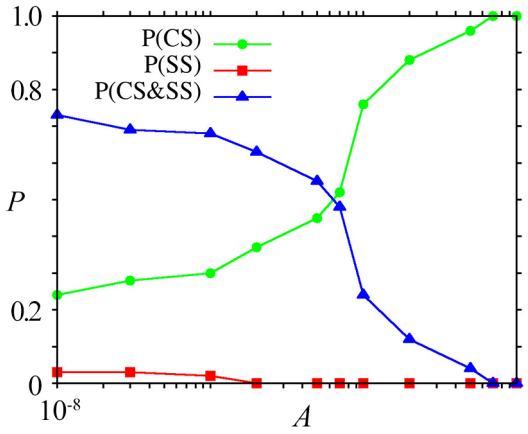

Fig 3. Probabilities of settling chimera states P(CS), solitary state regime P(SS), and combined structure regime P(CS&SS) in the network of FitzHugh–Nagumo oscillators versus the noise intensity A. The dependences are plotted using 100 different sets of initial conditions. Other parameters: $\varepsilon = 0.05$, $a = 0.5$, $R = 105$, $N = 300$ (color online)

in the ensemble (Fig. 4, *b*, *c*).

3. Impact of noise on solitary states

Let us analyze the influence of independent sources of additive normal white noise on the dynamics of the ensemble of FitzHugh–Nagumo oscillators (1) at values of the ensemble control parameters that correspond to the establishment of a regime of solitary states in the region of weak and strong coupling (see Fig. 1, blue areas).

Fig. 5 shows the distribution of the values of the correlation coefficient (4) in accordance with the regime maps shown in Fig. 1. It can be seen that in the region that corresponds to the presence of solitary nodes in the system, the cross-correlation coefficient averaged over the ensemble is $C \approx 0.96$ (compare Fig. 1 and Fig. 5). This value of C corresponds to the presence of

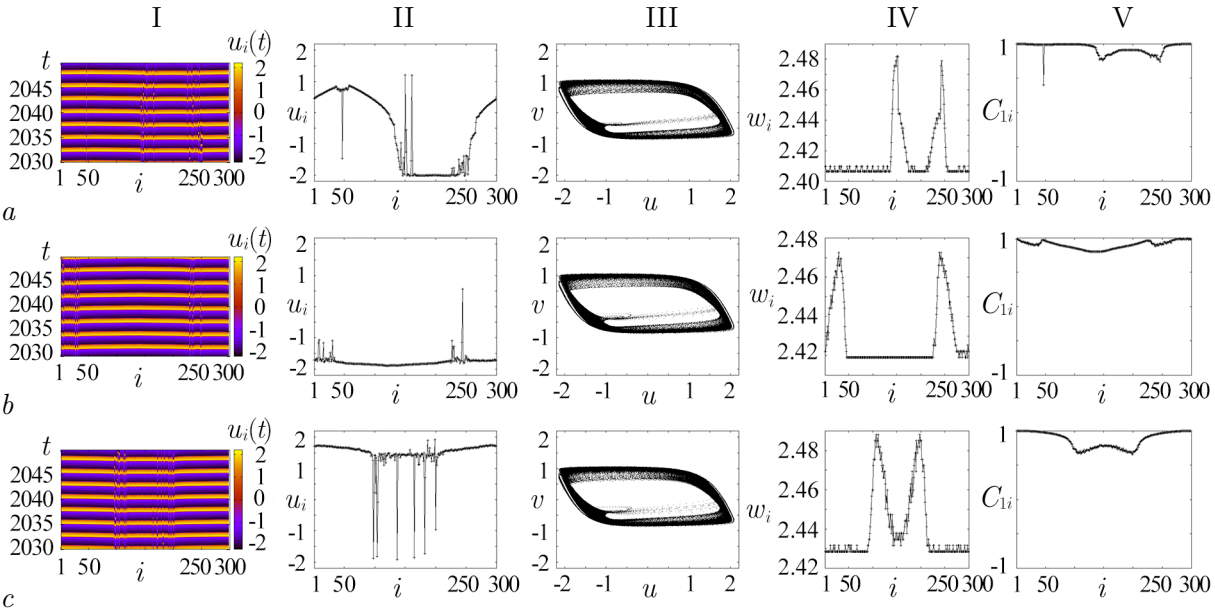

Fig 4. Dynamics of the network of nonlocally coupled FitzHugh–Nagumo oscillators for different values of the noise intensity: $A = 10^{-7}$ (*a*), 10^{-6} (*b*), 10^{-5} (*c*). Space-time diagrams (column I), snapshots (column II), projections of a multidimensional attractor on the (u, v) plane (column III), mean phase velocity profiles (column IV), cross-correlation coefficient profiles (column V). Other parameters and initial conditions corresponds to the structure in Fig. 2, *c* (color online)

a small number of solitary nodes in the system. As mentioned earlier, the correlation coefficient can only qualitatively display changes in the number of solitary nodes with increasing intensity of additive noise, but it allows us to monitor changes in the region of existence of solitary states.

In this regard, the distribution of values of averaged cross-correlation coefficients at different intensities of additive noise was constructed for one realization of random initial conditions of ensemble elements (Fig. 6). As can be seen, both regions of existence of solitary states decrease with increasing noise intensity. However, the region that is in the weak coupling range is more resistant to external influences (Fig. 6, *a*–*d*) than the one that is in the strong coupling range (fig. 6, *e*–*h*). Studies have shown that the region in which solitary state modes are observed in weak coupling completely disappears at $A \approx 7 \cdot 10^{-4}$, while in the case of strong coupling, a noise intensity one order of magnitude less than $A \approx 7 \cdot 10^{-5}$ so that solitary nodes are not observed in the ensemble.

For a more detailed study of the influence of additive noise on solitary states in a ring of nonlocally coupled FitzHugh–Nagumo oscillators, the dependence of the average number of solitary nodes on the coupling strength between elements and the intensity of additive noise was analyzed for fixed values of the ϕ parameter in the range of weak (Fig. 7, *a*) and strong coupling (Fig. 7, *b*). In this case, one realization of randomly distributed initial values of dynamic variables and ten different realizations of independent white Gaussian noise sources were used. As you can see, with a weak coupling the number of solitary nodes is less than with a strong coupling (compare the range of colorboxes of N_S in Fig. 7, *a* and 7, *b*). Moreover, the dependence of the number of solitary nodes on σ and A in the weak coupling interval, having a dome-shaped shape, is qualitatively reminiscent of the dependences that were observed in the rings of nonlocally coupled Lozi maps studied in the work [48]. The region of existence of solitary states in the case of strong coupling has a more linear left boundary (see Fig. 7, *b*). However, in all cases, an increase in the noise intensity leads predominantly to a decrease in the number of solitary nodes and the range of parameter values σ in which they are observed. Only in the case of weak coupling at $\sigma \approx 0.119$ can one observe that at $A = 0$ the number of solitary nodes tends to 0, and at $A > 0$ it can be at the level of $P \approx 0.006$ (which corresponds to the presence of two or three solitary nodes in the ensemble), however, when $A > 0.002$ the value of N_S again decreases to 0 (see Fig. 7, *a*) . The same is observed in the distribution maps of the average cross-correlation coefficient for the case of weak coupling, when, with increasing noise intensity, the region of existence of solitary states decreased and slightly shifted to the right towards larger σ values (see Fig. 6, *a*–*d*).

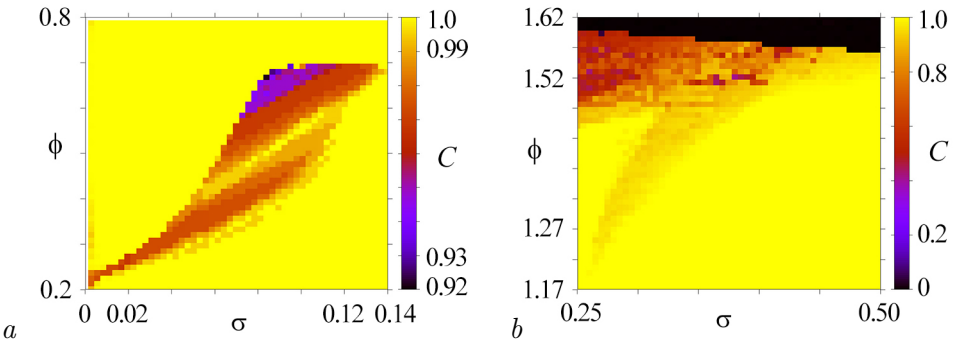

Fig 5. Distributions of averaged cross-correlation coefficient (4) values in the noise-free network (1) for weak (*a*) and strong (*b*) coupling. Other parameters: $\varepsilon = 0.05$, $a_0 = 0.5$, $R = 105$, $N = 300$, $A = 0$ (color online)

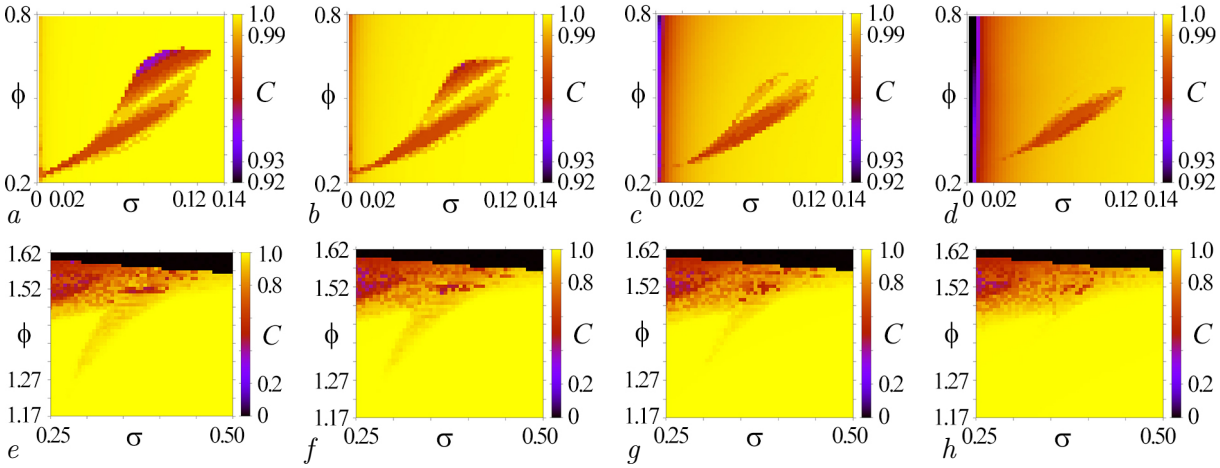

Fig 6. Distribution diagrams for the averaged cross-correlation coefficient (4) in the network (1) in the (σ, ϕ) parameter plane for weak $(a–d)$ and strong $(e–h)$ coupling for different values of the noise intensity: $A = 0.000005$ (a), 0.000025 (b), 0.000100 (c), 0.000200 (d), 0.000005 (e), 0.000010 (f), 0.000025 (g), 0.000050 (h). Other parameters: $\varepsilon = 0.05$, $a_0 = 0.5$, $R = 105$, $N = 300$ (color online)

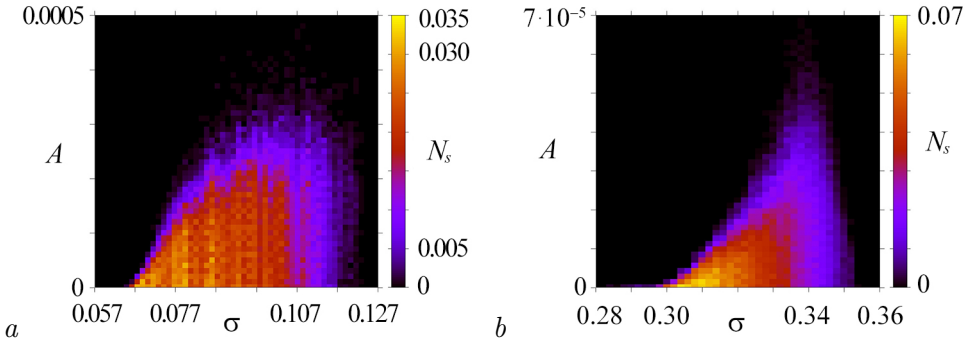

Fig 7. Mean normalized number of solitary nodes N_S in the network of coupled FitzHugh–Nagumo oscillators in the (σ, A) parameter plane for weak (a) and strong (b) coupling and for fixed values of the parameter ϕ: 0.52 (a), 1.4 (b). Calculations were performed for a single realization of randomly distributed initial conditions of the dynamical variables and 10 different noise realizations ($M = 10$). Other parameters: $\varepsilon = 0.05$, $a_0 = 0.5$, $R = 105$, $N = 300$ (color online)

Conclusion

The paper presents the results of numerical simulation of the dynamics of an ensemble of nonlocally coupled FitzHugh–Nagumo oscillators in the presence of additive noise. To analyze the influence of noise, we selected the values of the control coupling parameters corresponding to the multistability region, in which, depending on the initial conditions, chimera states, solitary state modes and combined structures can be observed, as well as the corresponding existing in the ensemble of only the solitary state (in the range of weak and strong coupling).

It is shown that in the ring of nonlocally coupled FitzHugh–Nagumo oscillators, the effect of additive noise on regimes occurring in the multistability region leads to an increase in the probability of establishing only chimera states, while the probabilities of observing other regimes decrease to zero with increasing noise intensity. Thus, in the presence of additive noise influence, chimera states manifest themselves as more stable and dominant structures among all others coexisting in the ensemble.

When additive noise is introduced into the ensemble under study, which in the absence

of noise exhibits only solitary state, an increase in the noise intensity in the general case leads to a decrease in the range of coupling parameters in which solitary states are observed and to a decrease in the number of solitary nodes, which also occurred in rings of nonlocally coupled Lozi maps [48]. However, in a ring of nonlocally coupled FitzHugh–Nagumo oscillators, in the case of weak coupling, the introduction of additive noise can promote the appearance of solitary states with a coupling strength approximately 0.04 greater than the maximum coupling strength at which solitary nodes were observed in the noise-free ensemble.

References

1. Benzi R, Sutera A, Vulpiani A. The mechanism of stochastic resonance. Journal of Physics A: Mathematical and General. 1981;14(11):L453–L457. DOI: 10.1088/0305-4470/14/11/006.
2. Horsthemke W, Lefever R. Noise-induced transitions in physics, chemistry, and biology. In: Noise-Induced Transitions. Vol. 15 of Springer Series in Synergetics. Berlin, Heidelberg: Springer; 1984. P. 164–200. DOI: 10.1007/3-540-36852-3_7.
3. Neiman A. Synchronizationlike phenomena in coupled stochastic bistable systems. Physical Review E. 1994;49(4):3484–3487. DOI: 10.1103/PhysRevE.49.3484.
4. Arnold L. Random dynamical systems. In: Johnson R, editor. Dynamical Systems. Vol. 1609 of Lecture Notes in Mathematics. Berlin, Heidelberg: Springer; 1995. P. 1–43. DOI: 10.1007/BFb0095238.
5. Pikovsky AS, Kurths J. Coherence resonance in a noise-driven excitable system. Physical Review Letters. 1997;78(5):775–778. DOI: 10.1103/PhysRevLett.78.775.
6. Anishchenko VS, Neiman AB, Moss F, Shimansky-Geier L. Stochastic resonance: noise-enhanced order. Phys. Usp. 1999;42(1):7–36. DOI: 10.1070/PU1999v042n01ABEH000444.
7. Goldobin DS, Pikovsky A. Synchronization and desynchronization of self-sustained oscillators by common noise. Physical Review E. 2005;71(4):045201. DOI: 10.1103/PhysRevE.71.045201.
8. McDonnell MD, Ward LM. The benefits of noise in neural systems: bridging theory and experiment. Nature Reviews Neuroscience. 2011;12(7):415–425. DOI: 10.1038/nrn3061.
9. Schimansky-Geier L, Herzel H. Positive Lyapunov exponents in the Kramers oscillator. Journal of Statistical Physics. 1993;70(1–2):141–147. DOI: 10.1007/BF01053959.
10. Shulgin B, Neiman A, Anishchenko V. Mean switching frequency locking in stochastic bistable systems driven by a periodic force. Physical Review Letters. 1995;75(23):4157–4160. DOI: 10.1103/PhysRevLett.75.4157.
11. Arnold L, Namachchivaya NS, Schenk-Hoppé KR. Toward an understanding of stochastic Hopf bifurcation: A case study. International Journal of Bifurcation and Chaos. 1996;6(11):1947–1975. DOI: 10.1142/S0218127496001272.
12. Han SK, Yim TG, Postnov DE, Sosnovtseva OV. Interacting coherence resonance oscillators. Physical Review Letters. 1999;83(9):1771–1774. DOI: 10.1103/PhysRevLett.83.1771.
13. Bashkirtseva I, Ryashko L, Schurz H. Analysis of noise-induced transitions for Hopf system with additive and multiplicative random disturbances. Chaos, Solitons & Fractals. 2009;39(1):72–82. DOI: 10.1016/j.chaos.2007.01.128.
14. Gammaitoni L, Marchesoni F, Menichella-Saetta E, Santucci S. Stochastic resonance in bistable systems. Physical Review Letters. 1989;62(4):349–352. DOI: 10.1103/PhysRevLett.62.349.
15. Lindner B, Schimansky-Geier L. Analytical approach to the stochastic FitzHugh-Nagumo system and coherence resonance. Physical Review E. 1999;60(6):7270–7276. DOI: 10.1103/PhysRevE.60.7270.
16. Kuramoto Y, Battogtokh D. Coexistence of coherence and incoherence in nonlocally coup-

led phase oscillators. Nonlinear Phenomena in Complex Systems. 2002;5(4):380–385.
17. Abrams DM, Strogatz SH. Chimera states for coupled oscillators. Physical Review Letters. 2004;93(17):174102. DOI: 10.1103/PhysRevLett.93.174102.
18. Omelchenko I, Maistrenko Y, Hövel P, Schöll E. Loss of coherence in dynamical networks: Spatial chaos and chimera states. Physical Review Letters. 2011;106(23):234102. DOI: 10.1103/PhysRevLett.106.234102.
19. Panaggio MJ, Abrams DM. Chimera states: coexistence of coherence and incoherence in networks of coupled oscillators. Nonlinearity. 2015;28(3):R67. DOI: 10.1088/0951-7715/28/3/R67.
20. Zakharova A. Chimera Patterns in Networks: Interplay between Dynamics, Structure, Noise, and Delay. Cham: Springer; 2020. 233 p. DOI: 10.1007/978-3-030-21714-3.
21. Maistrenko Y, Penkovsky B, Rosenblum M. Solitary state at the edge of synchrony in ensembles with attractive and repulsive interactions. Physical Review E. 2014;89(6):060901. DOI: 10.1103/PhysRevE.89.060901.
22. Jaros P, Maistrenko Y, Kapitaniak T. Chimera states on the route from coherence to rotating waves. Physical Review E. 2015;91(2):022907. DOI: 10.1103/PhysRevE.91.022907.
23. Bogomolov SA, Slepnev AV, Strelkova GI, Schöll E, Anishchenko VS. Mechanisms of appearance of amplitude and phase chimera states in ensembles of nonlocally coupled chaotic systems. Communications in Nonlinear Science and Numerical Simulation. 2017;43:25–36. DOI: 10.1016/j.cnsns.2016.06.024.
24. Panaggio MJ, Abrams DM. Chimera states on a flat torus. Physical Review Letters. 2013;110(9):094102. DOI: 10.1103/PhysRevLett.110.094102.
25. Sawicki J, Omelchenko I, Zakharova A, Schöll E. Chimera states in complex networks: interplay of fractal topology and delay. The European Physical Journal Special Topics. 2017;226(9):1883–1892. DOI: 10.1140/epjst/e2017-70036-8.
26. Schöll E. Synchronization patterns and chimera states in complex networks: Interplay of topology and dynamics. The European Physical Journal Special Topics. 2016;225(6–7):891–919. DOI: 10.1140/epjst/e2016-02646-3.
27. Schöll E. Chimeras in physics and biology: Synchronization and desynchronization of rhythms. In: Hacker J, Lengauer T, editors. Zeit in Natur und Kultur: Vorträge anlässlich der Jahresversammlung am 20. und 21. September 2019 in Halle (Saale). Stuttgart: Wissenschaftliche Verlagsgesellschaft; 2021. P. 67–95. DOI: 10.26164/leopoldina_10_00275.
28. Semenova N, Zakharova A, Schöll E, Anishchenko V. Does hyperbolicity impede emergence of chimera states in networks of nonlocally coupled chaotic oscillators? Europhysics Letters. 2015;112(4):40002. DOI: 10.1209/0295-5075/112/40002.
29. Shima S, Kuramoto Y. Rotating spiral waves with phase-randomized core in nonlocally coupled oscillators. Physical Review E. 2004;69(3):036213. DOI: 10.1103/PhysRevE.69.036213.
30. Ulonska S, Omelchenko I, Zakharova A, Schöll E. Chimera states in networks of Van der Pol oscillators with hierarchical connectivities. Chaos: An Interdisciplinary Journal of Nonlinear Science. 2016;26(9):094825. DOI: 10.1063/1.4962913.
31. Zakharova A, Kapeller M, Schöll E. Chimera death: Symmetry breaking in dynamical networks. Physical Review Letters. 2014;112(15):154101. DOI: 10.1103/PhysRevLett.112.154101.
32. Menck PJ, Heitzig J, Kurths J, Schellnhuber HJ. How dead ends undermine power grid stability. Nature Communications. 2014;5(1):3969. DOI: 10.1038/ncomms4969.
33. Motter AE, Myers SA, Anghel M, Nishikawa T. Spontaneous synchrony in power-grid networks. Nature Physics. 2013;9(3):191–197. DOI: 10.1038/nphys2535.

34. Wang B, Suzuki H, Aihara K. Enhancing synchronization stability in a multi-area power grid. Scientific Reports. 2016;6(1):26596. DOI: 10.1038/srep26596.
35. Hong S, Chun Y. Efficiency and stability in a model of wireless communication networks. Social Choice and Welfare. 2010;34(3):441–454. DOI: 10.1007/s00355-009-0409-1.
36. González-Avella JC, Cosenza MG, San Miguel M. Localized coherence in two interacting populations of social agents. Physica A: Statistical Mechanics and its Applications. 2014;399: 24–30. DOI: 10.1016/j.physa.2013.12.035.
37. Bansal K, Garcia JO, Tompson SH, Verstynen T, Vettel JM, Muldoon SF. Cognitive chimera states in human brain networks. Science Advances. 2019;5(4):eaau8535. DOI: 10.1126/sciadv.aau8535.
38. Majhi S, Bera BK, Ghosh D, Perc M. Chimera states in neuronal networks: A review. Physics of Life Reviews. 2019;28:100–121. DOI: 10.1016/j.plrev.2018.09.003.
39. Schöll E. Partial synchronization patterns in brain networks. Europhysics Letters. 2022; 136(1):18001. DOI: 10.1209/0295-5075/ac3b97.
40. Levy R, Hutchison WD, Lozano AM, Dostrovsky JO. High-frequency synchronization of neuronal activity in the subthalamic nucleus of parkinsonian patients with limb tremor. J. Neurosci. 2000;20(20):7766–7775. DOI: 10.1523/JNEUROSCI.20-20-07766.2000.
41. Rattenborg NC, Amlaner CJ, Lima SL. Behavioral, neurophysiological and evolutionary perspectives on unihemispheric sleep. Neurosci. Biobehav. Rev. 2000;24(8):817–842. DOI: 10.1016/s0149-7634(00)00039-7.
42. Funahashi S, Bruce CJ, Goldman-Rakic PS. Neuronal activity related to saccadic eye movements in the monkey's dorsolateral prefrontal cortex. J. Neurophysiol. 1991;65(6):1464–1483. DOI: 10.1152/jn.1991.65.6.1464.
43. Swindale NV. A model for the formation of ocular dominance stripes. Proc. R. Soc. Lond. B. 1980;208(1171):243–264. DOI: 10.1098/rspb.1980.0051.
44. Andrzejak RG, Rummel C, Mormann F, Schindler K. All together now: Analogies between chimera state collapses and epileptic seizures. Scientific Reports. 2016;6(1):23000. DOI: 10.1038/srep23000.
45. Malchow A-K, Omelchenko I, Schöll E, Hövel P. Robustness of chimera states in nonlocally coupled networks of nonidentical logistic maps. Physical Review E. 2018;98(1):012217. DOI: 10.1103/PhysRevE.98.012217.
46. Bukh AV, Slepnev AV, Anishchenko VS, Vadivasova TE. Stability and noise-induced transitions in an ensemble of nonlocally coupled chaotic maps. Regular and Chaotic Dynamics. 2018;23(3):325–338. DOI: 10.1134/S1560354718030073.
47. Rybalova EV, Klyushina DY, Anishchenko VS, Strelkova GI. Impact of noise on the amplitude chimera lifetime in an ensemble of nonlocally coupled chaotic maps. Regular and Chaotic Dynamics. 2019;24(4):432–445. DOI: 10.1134/S1560354719040051.
48. Rybalova E, Schöll E, Strelkova G. Controlling chimera and solitary states by additive noise in networks of chaotic maps. Journal of Difference Equations and Applications. 2022:1–22. DOI: 10.1080/10236198.2022.2118580.
49. Rybalova E, Muni S, Strelkova G. Transition from chimera/solitary states to traveling waves. Chaos: An Interdisciplinary Journal of Nonlinear Science. 2023;33(3):033104. DOI: 10.1063/5.0138207.
50. Nechaev VA, Rybalova EV, Strelkova GI. Influence of parameters inhomogeneity on the existence of chimera states in a ring of nonlocally coupled maps. Izvestiya VUZ. Applied Nonlinear Dynamics. 2021;29(6):943–952 (in Russian). DOI: 10.18500/0869-6632-2021-29-6-943-952.
51. Nikishina NN, Rybalova EV, Strelkova GI, Vadivasova TE. Destruction of cluster structures

in an ensemble of chaotic maps with noise-modulated nonlocal coupling. Regular and Chaotic Dynamics. 2022;27(2):242–251. DOI: 10.1134/S1560354722020083.
52. Omelchenko I, Provata A, Hizanidis J, Schöll E, Hövel P. Robustness of chimera states for coupled FitzHugh-Nagumo oscillators. Physical Review E. 2015;91(2):022917. DOI: 10.1103/PhysRevE.91.022917.
53. Semenova N, Zakharova A, Anishchenko V, Schöll E. Coherence-resonance chimeras in a network of excitable elements. Physical Review Letters. 2016;117(1):014102. DOI: 10.1103/PhysRevLett.117.014102.
54. Zakharova A, Loos S, Siebert J, Gjurchinovski A, Schöll E. Chimera patterns: influence of time delay and noise. IFAC-PapersOnLine. 2015;48(18):7–12. DOI: 10.1016/j.ifacol.2015.11.002.
55. Loos SAM, Claussen JC, Schöll E, Zakharova A. Chimera patterns under the impact of noise. Physical Review E. 2016;93(1):012209. DOI: 10.1103/PhysRevE.93.012209.
56. Wu H, Dhamala M. Dynamics of Kuramoto oscillators with time-delayed positive and negative couplings. Physical Review E. 2018;98(3):032221. DOI: 10.1103/PhysRevE.98.032221.
57. Jaros P, Brezetsky S, Levchenko R, Dudkowski D, Kapitaniak T, Maistrenko Y. Solitary states for coupled oscillators with inertia. Chaos: An Interdisciplinary Journal of Nonlinear Science. 2018;28(1):011103. DOI: 10.1063/1.5019792.
58. Berner R, Polanska A, Schöll E, Yanchuk S. Solitary states in adaptive nonlocal oscillator networks. The European Physical Journal Special Topics. 2020;229(12–13):2183–2203. DOI: 10.1140/epjst/e2020-900253-0.
59. Semenova NI, Rybalova EV, Strelkova GI, Anishchenko VS. "Coherence–incoherence" transition in ensembles of nonlocally coupled chaotic oscillators with nonhyperbolic and hyperbolic attractors. Regular and Chaotic Dynamics. 2017;22(2):148–162. DOI: 10.1134/S1560354717020046.
60. Semenova N, Vadivasova T, Anishchenko V. Mechanism of solitary state appearance in an ensemble of nonlocally coupled Lozi maps. The European Physical Journal Special Topics. 2018;227(10–11):1173–1183. DOI: 10.1140/epjst/e2018-800035-y.
61. Schülen L, Ghosh S, Kachhvah AD, Zakharova A, Jalan S. Delay engineered solitary states in complex networks. Chaos, Solitons & Fractals. 2019;128:290–296. DOI: 10.1016/j.chaos.2019.07.046.
62. Mikhaylenko M, Ramlow L, Jalan S, Zakharova A. Weak multiplexing in neural networks: Switching between chimera and solitary states. Chaos: An Interdisciplinary Journal of Nonlinear Science. 2019;29(2):023122. DOI: 10.1063/1.5057418.
63. Rybalova E, Anishchenko VS, Strelkova GI, Zakharova A. Solitary states and solitary state chimera in neural networks. Chaos: An Interdisciplinary Journal of Nonlinear Science. 2019;29(7):071106. DOI: 10.1063/1.5113789.
64. Schülen L, Janzen DA, Medeiros ES, Zakharova A. Solitary states in multiplex neural networks: Onset and vulnerability. Chaos, Solitons & Fractals. 2021;145:110670. DOI: 10.1016/j.chaos.2021.110670.
65. Taher H, Olmi S, Schöll E. Enhancing power grid synchronization and stability through time-delayed feedback control. Physical Review E. 2019;100(6):062306. DOI: 10.1103/PhysRevE.100.062306.
66. Hellmann F, Schultz P, Jaros P, Levchenko R, Kapitaniak T, Kurths J, Maistrenko Y. Network-induced multistability through lossy coupling and exotic solitary states. Nature Communications. 2020;11(1):592. DOI: 10.1038/s41467-020-14417-7.
67. Berner R, Yanchuk S, Schöll E. What adaptive neuronal networks teach us about power

grids. Physical Review E. 2021;103(4):042315. DOI: 10.1103/PhysRevE.103.042315.
68. Kapitaniak T, Kuzma P, Wojewoda J, Czolczynski K, Maistrenko Y. Imperfect chimera states for coupled pendula. Scientific Reports. 2014;4(1):6379. DOI: 10.1038/srep06379.
69. Fried I, MacDonald KA, Wilson CL. Single neuron activity in human hippocampus and amygdala during recognition of faces and objects. Neuron. 1997;18(5):753–765. DOI: 10.1016/s0896-6273(00)80315-3.
70. Kreiman G, Koch C, Fried I. Category-specific visual responses of single neurons in the human medial temporal lobe. Nature Neuroscience. 2000;3(9):946–953. DOI: 10.1038/78868.
71. Rose D. Some reflections on (or by?) grandmother cells. Perception. 1996;25(8):881–886. DOI: 10.1068/p250881.
72. Quiroga RQ, Reddy L, Kreiman G, Koch C, Fried I. Invariant visual representation by single neurons in the human brain. Nature. 2005;435(7045):1102–1107. DOI: 10.1038/nature03687.
73. Xin Y, Zhong L, Zhang Y, Zhou T, Pan J, Xu N-L. Sensory-to-category transformation via dynamic reorganization of ensemble structures in mouse auditory cortex. Neuron. 2019;103(5):909–921. DOI: 10.1016/j.neuron.2019.06.004.
74. Franović I, Eydam S, Semenova N, Zakharova A. Unbalanced clustering and solitary states in coupled excitable systems. Chaos: An Interdisciplinary Journal of Nonlinear Science. 2022;32(1):011104. DOI: 10.1063/5.0077022.
75. Rybalova E, Strelkova G. Response of solitary states to noise-modulated parameters in nonlocally coupled networks of Lozi maps. Chaos: An Interdisciplinary Journal of Nonlinear Science. 2022;32(2):021101. DOI: 10.1063/5.0082431.
76. Omelchenko I, Omel'chenko OE, Hövel P, Schöll E. When nonlocal coupling between oscillators becomes stronger: Patched synchrony or multichimera states. Physical Review Letters. 2013;110(22):224101. DOI: 10.1103/PhysRevLett.110.224101.
77. FitzHugh R. Impulses and physiological states in theoretical models of nerve membrane. Biophysical Journal. 1961;1(6):445–466. DOI: 10.1016/s0006-3495(61)86902-6.
78. Nagumo J, Arimoto S, Yoshizawa S. An active pulse transmission line simulating nerve axon. Proceedings of the IRE. 1962;50(10):2061–2070. DOI: 10.1109/JRPROC.1962.288235.